Using anisotropy of magnetic susceptibility to better constrain the tilt correction in paleomagnetism: A case study from southern Peru

Pierrick Roperch, Victor Carlotto, Annick Chauvin

Using anisotropy of magnetic susceptibility to better constrain the tilt correction in paleomagnetism: A case study from southern Peru

Pierrick Roperch,[1,2] Victor Carlotto,[3,4] and Annick Chauvin[2]

Received 4 December 2009; revised 28 April 2010; accepted 22 June 2010; published 13 November 2010.

[1] We report a combined study of anisotropy of low field magnetic susceptibility (AMS) and paleomagnetism from 16 sites in a sedimentary sequence of Eocene–early Oligocene red beds in southern Peru. Incipient tectonic strain is recorded during the early stages of deformation. Nonhorizontal magnetic lineation in geographic coordinate suggests either noncylindrical folding and/or interference of two phases of compressive deformation and tectonic rotation. Applying the classic tilt correction results in significant dispersion in paleomagnetic declinations and apparent clockwise and counterclockwise relative tectonic rotations. A dispersion in the orientation of the magnetic lineation also arises from a simple classic tilt correction inducing apparent local rotation in paleostress determination. The magnetic lineation is a good proxy to detect a complex history of folding when the finite strain is not large enough to reset the magnetic fabric acquired during the early stages of deformation and when detailed geological field mapping is not available or not possible. In the present study, a double correction rotating first the lineation to the horizontal reduces significantly the dispersion of the paleomagnetic data with respect to conventional tilt correction (Fisher parameter k increases from 14 to 35). The interest of this double correction must obviously be evaluated for each study according to the complexity of the folding and the intensity of the deformation. Assuming a mean age of 40 Ma for the sedimentary sequence, no significant rotation (−4.5° ± 8.4) is observed in this area of the Peruvian Andes.

Citation: Roperch, P., V. Carlotto, and A. Chauvin (2010), Using anisotropy of magnetic susceptibility to better constrain the tilt correction in paleomagnetism: A case study from southern Peru, *Tectonics*, *29*, TC6005, doi:10.1029/2009TC002639.

1. Introduction

[2] In many paleomagnetic studies, tectonic control on local structures such as dipping fold axis is often poorly determined and bedding correction is applied around an horizontal axis. It is well known that this correction may lead to apparent local rotation [*MacDonald*, 1980; *Perroud and Cobbold*, 1984]. Anisotropy of low field magnetic susceptibility is a versatile petrofabric tool [*Rochette et al.*, 1992; *Borradaile and Henry*, 1997] and anisotropy of low field magnetic susceptibility (AMS) data have been widely acquired, especially with the advancement of technology like the spinner kappabridges from Agico. Even though an information about sedimentary processes may be recognized in some cases [*Rees*, 1965; *Aubourg et al.*, 2004], the majority of AMS studies yield strong evidence that triaxial AMS ellipsoids in sediments are mainly controlled by compaction and tectonic strain. *Cifelli et al.* [2009] suggest that AMS is a useful and often unique method to study the deformation history of apparently undeformed sediments. In a study of marine Cenozoic clays from Greece, *Kissel et al.* [1986] demonstrated that the magnetic lineation develop parallel to fold axes. Grouping of principal axis of AMS ellipsoids (Kmax) parallel to the general trend of folds has been observed in several studies [*Robion et al.*, 1995, *Sagnotti et al.*, 1999; *Weaver et al.*, 2004, *Huang et al.*, 2004]. The timing of the acquisition of the magnetic fabric is however disputed. *Graham* [1966] indicated that a change from sedimentary to tectonic fabric is more likely to append within unconsolidated rocks. In compressional setting, several studies indicate that the magnetic fabric is likely acquired during the early stages of diagenesis and deformation (see *Pares et al.* [1999] and *Frizon de Lamotte et al.* [2002] for a review). This lineation is usually termed Layer Parallel Shortening (LPS). A recent study comparing magnetic fabric and paleostress data also validates the reliability of AMS as paleostress indicator in compressive settings [*Soto et al.*, 2009]. Although lineations due to LPS are the most common cases, *Aubourg et al.* [1999, and references therein] report also examples of magnetic lineations in the direction of tectonic transport as the result of simple shear during the early building of the thrust sheets. Magnetic lineations in the downdip directions of the foliation plane and in the direction of the transport direction are also usually observed in ignimbrites [*Paquereau et al.*, 2008].

[3] *Aubry et al.* [1996], *Coutand et al.* [1999] and *Roperch et al.* [2000] reported AMS data from the central Andes showing a relation between the tectonic rotations and the orientation of the magnetic lineations. These results were interpreted as evidence of rotations around vertical axes of fold axes during Andean deformation and oroclinal bending.

[4] Here, we report a paleomagnetic study from an Eocene to early Oligocene continental red bed sequence in southern

[1]IRD, LMTG, Toulouse, France.
[2]Géosciences Rennes, Rennes, France.
[3]INGEMMET, San Borja, Lima, Peru.
[4]UNSAAC, Cusco, Peru.

0278-7407/10/2009TC002639

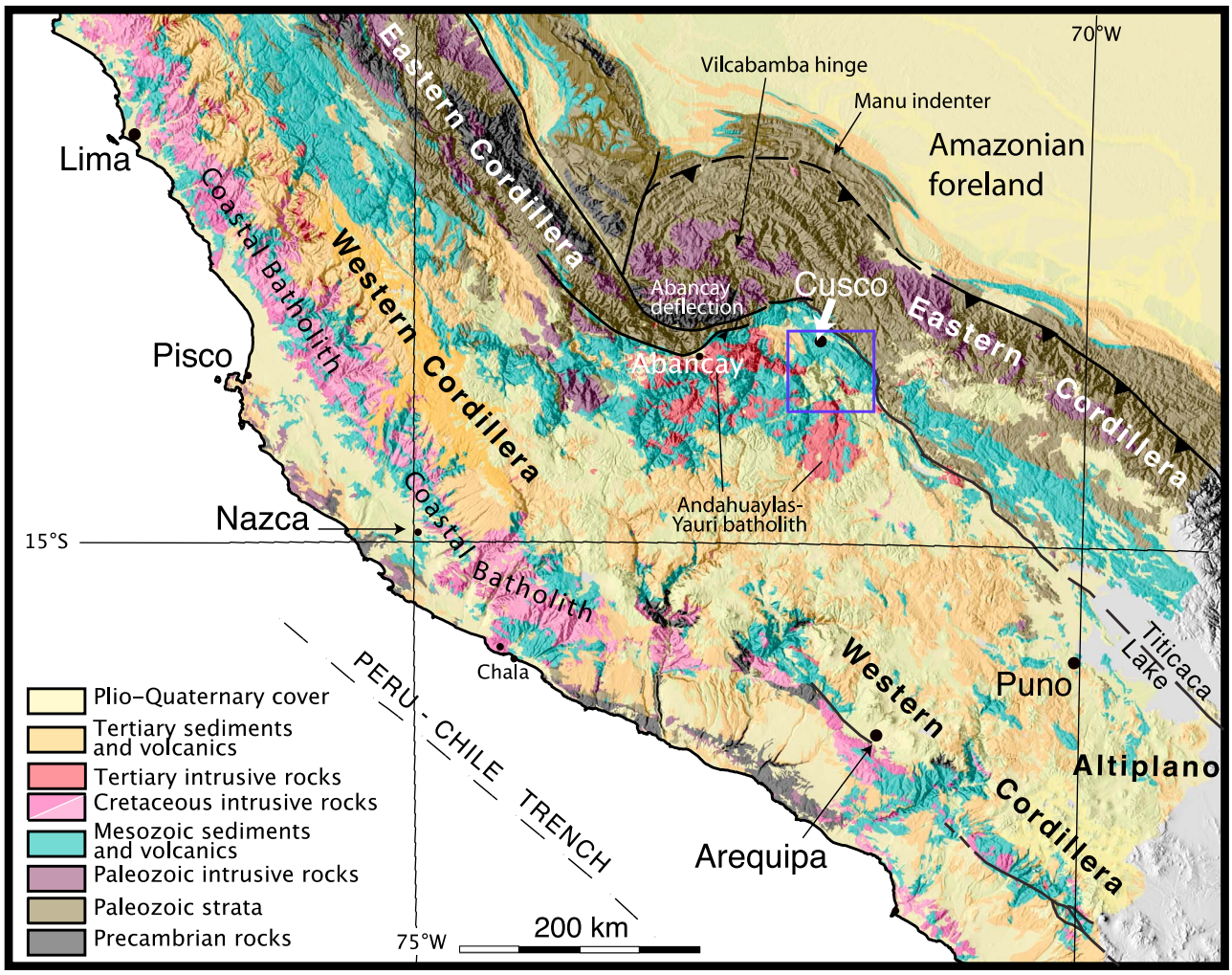

Figure 1. Geological map of southern Peru showing the location of the study area (blue square) southwest of the town of Cusco. The study area is located west of the boundary between the Eastern Cordillera and the northeastern Altiplano. The Altiplano is also bounded to the north by the Abancay deflection. Simplified geological map modified from the 1/1,000,000 digital geological map by INGEMMET and *Roperch et al.* [2006].

Peru (Figure 1) south of the town of Cusco. In the present study, AMS lineations are within the bedding planes but they are not always horizontal as expected with cylindrical folding around horizontal axes. We show that the AMS lineations provide evidence for complex folding and that the AMS may be used to further correct the paleomagnetic characteristic directions.

2. Regional Geology and Paleomagnetic Sampling

[5] In southern Peru, the Altiplano contains major syntectonic Cenozoic continental sedimentary basins. The sedimentary San Jerónimo Group corresponds to Eocene to early Oligocene sequences, found to the south and southwest of the town of Cusco (Figure 2). The San Jerónimo Group consists of two main formations (Kayra and Soncco), with a total thickness of ~4,500 m, made up of red bed terrigenous (sandstone, shale, pelitic sandstone, and volcanic microconglomerate) strata interbedded with tuffaceous horizons near the top. The San Jerónimo Group unconformably overlies strata with plant fossils of Paleocene to early Eocene age and K-Ar and $^{40}Ar/^{39}Ar$ ages of 29.9 ± 1.4 Ma and 30.84 ± 0.83 have been found in the uppermost tuffaceous layers of the Soncco formation (near site 2 in Figure 2) [*Carlotto*, 1998; *Fornari et al.*, 2002]. The coarsening-upward characteristics of the sequence, with alluvial and fluvial conglomerates dominated by volcanic and plutonic clasts at the top, are interpreted to reflect topographic rejuvenation of the source regions in response to increasing regional tectonic uplift. Sediments were deposited in a piggyback style basin environment [*Carlotto*, 1998]. *Carlier et al.* [2005] indicate

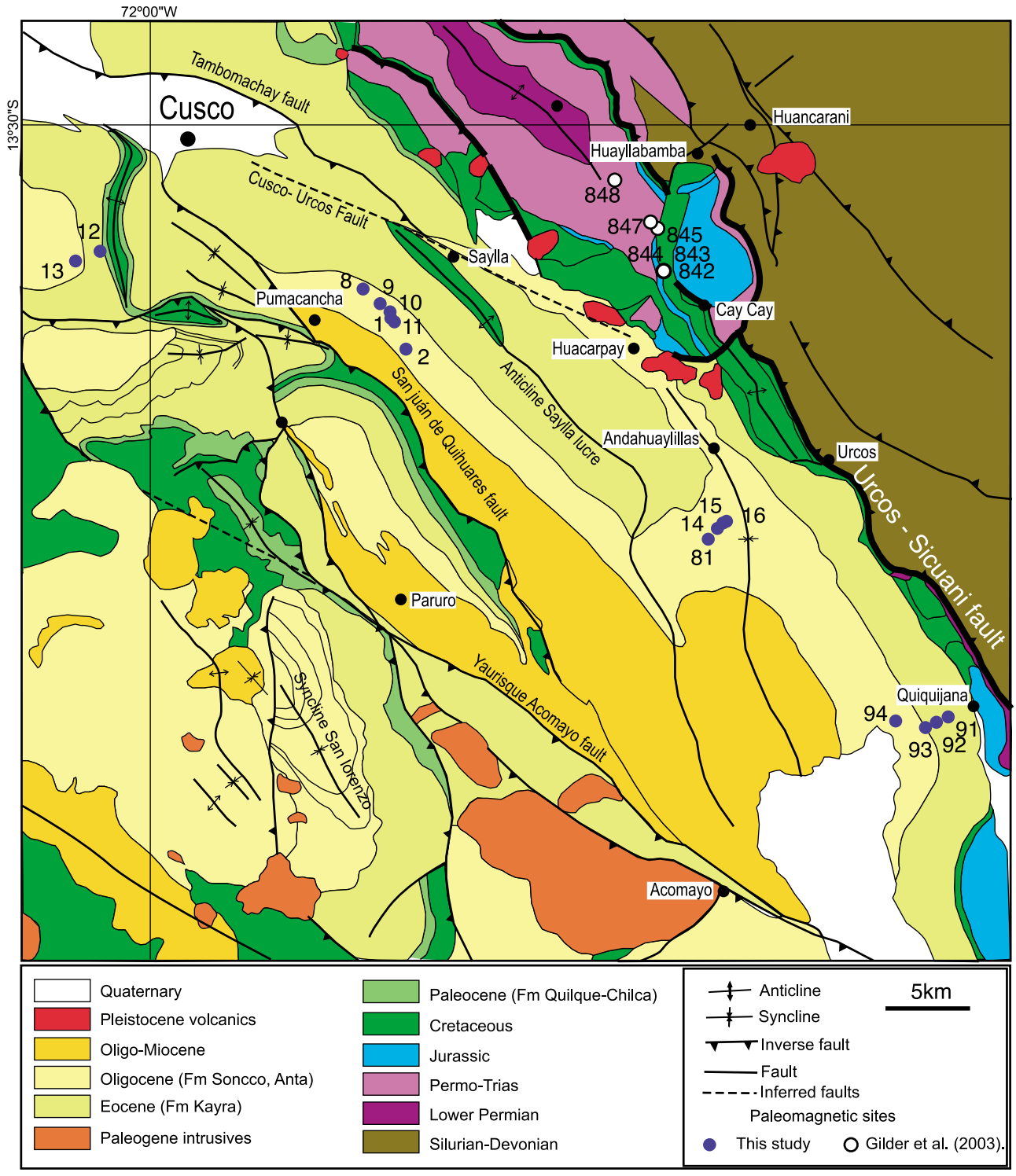

Figure 2. Geological map of the Cusco region and paleomagnetic sampling sites indicated by blue circles. Paleomagnetic sites from *Gilder et al.* [2003] are shown with white circles.

that the Urcos-Sicuani fault system separates two blocks with different underlying lithospheres. The Tertiary red beds are found on the western block while the eastern block comprises Paleozoic and highly deformed Mesozoic rocks. Large counterclockwise rotations were found in late Permian to Jurassic rocks sampled within the complex fault system limiting the two blocks [*Gilder et al.*, 2003].

[6] Samples were taken at four different localities. South of Cusco, the Soncco formation was sampled by six sites (8,9,10,1,11,2) distributed along a road from an elevation of

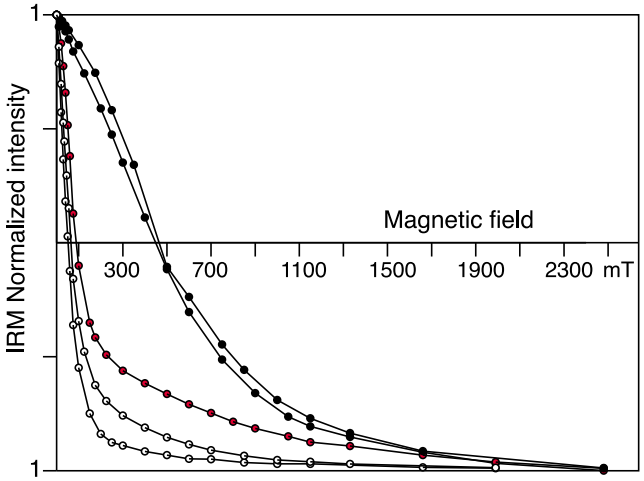

Figure 3. Backfield Isothermal Remanent Magnetization (IRM) acquisition after saturation with a field of 2500 mT. Black circles correspond to two samples from the Lower Kayra formation showing hematite as the main magnetic carrier. White circles correspond to two samples in the Soncco formation with magnetite and hematite as the magnetic carriers. Red circles correspond to a sample of the Kayra formation after heating in air in the laboratory up to 680°C with formation of magnetite.

about 3400 m up to 4200 m. The sequence is dipping toward the southwest by about 60°. Thus the sampled section has a thickness of more than 1000 m of the Soncco formation. The uppermost site (site 2) is slightly above the tuff for which *Carlotto* [1998] reported an age 29.9 ± 1.4 Ma. About 20 km to the southeast of the previous section, four sites (14,15,16,81) were also drilled in the Soncco formation. About 16 km farther south and east of Quiquijana, four sites (91,92,93,94) were drilled in the Kayra formation. Site 91 is near the base of the sequence and site 94 is about 2000 m upward in the sequence, either in the upper part of the Kayra or in the lower part of the Soncco formation. Finally two sites (12 and 13) were drilled in red beds southwest of Cusco and they are located on the western limb of a NS anticline oblique to the general WNW-ESE observed in the region suggesting possible interference of two phases of folding that will be later discussed. These 16 sites are in the same structural block bounded to the east by the Urcos-Sicuani-Ayaviri fault and to the west by the Yaurisque Acomayo fault.

3. Paleomagnetic Results

[7] Samples were drilled in the field and later cut to 2.2 cm specimens in the paleomagnetic laboratory of Géosciences Rennes. Natural remanent magnetizations were measured with a 2G cryogenic magnetometer. Thermal demagnetizations were performed with a MMTD furnace or a Schonstedt furnace. Anisotropy of magnetic susceptibility was measured with an AGICO KLY3S kappabridge. Isothermal Remanent Magnetization (IRM) was acquired with an ASC pulse magnetometer using a maximum applied field of 2.5T.

3.1. Magnetic Properties

[8] Samples from sites in the lowermost Kayra formation (sites 91, 92, 93, 94 near Quiquijana) have hematite as the main magnetic carrier as shown by IRM acquisition and thermal demagnetization of the NRM showing unblocking temperatures above 650°C (Figures 3 and 4). Magnetic susceptibility is in the range 1 to 2 10^{-4} SI except at site 12. From the geological map, site 12 belongs also to the Kayra formation but its high magnetic susceptibility suggests a richest source of volcanoclastic sediments and the magnetic behavior of these samples is similar to those of the Soncco formation. Upon heating in the laboratory during thermal demagnetization in air, samples from sites near Quiquijana exhibit up to tenfold increase in magnetic susceptibility from 500°C to 680°C. IRM acquisition in samples previously thermally demagnetized in the laboratory confirm that the susceptibility increase is associated with the formation of magnetic mineral with lower coercivities likely magnetite (Figure 3). In the overlying Soncco formation, magnetic susceptibility is higher and in the range 10^{-3}–10^{-2} SI and this increase in susceptibility corresponds to an input of volcanoclastic sediments due to erosion of the Eocene arc located to the west. The magnetic susceptibility decreases upon heating for samples from the Soncco formation contrary to the behavior of samples from the Kayra formation. This decrease is likely associated with oxidation of magnetite and/or maghemite upon heating in the laboratory [*Cifelli et al.*, 2004].

3.2. Characteristic Directions

[9] Hematite is the single magnetic carrier in the Kayra formation with half of the magnetization remaining above 660°C (Figure 4) while samples from the Soncco formation have lower unblocking temperature with both magnetite and hematite as magnetic carrier (Figure 4). A secondary magnetization usually in the present-day field is removed by demagnetization below 300°C. The characteristic magnetization was determined by linear fit through the origin. Samples from all sites in the Soncco formation have all a reverse polarity while normal and reverse polarity is observed in the different sites of the Kayra formation. The record of both two polarities at different sites indicates that the magnetization is a primary magnetization acquired during deposition or early diagenesis and formation of hematite. Upon tilt correction, there is a significant decrease in the dispersion in inclination between the sites (in inclination only statistics, concentration parameter k increases from 5 to 41) but the dispersion in declination is still large (Figure 5) with a resulting *Fisher* [1953] k parameter of only 14 (Table 1). (See also Figure S1.)[1]

3.3. Anisotropy of Magnetic Susceptibility

[10] Triaxial ellipsoids are observed at most sites in red beds of the Soncco and Kayra formation. Although we cannot discard that paramagnetic minerals may control part of the magnetic anisotropy in samples from the Kayra formation, the high susceptibility of samples from the Soncco implies that magnetite and maghemite are the main carriers of

[1] Auxiliary materials are available with the HTML.

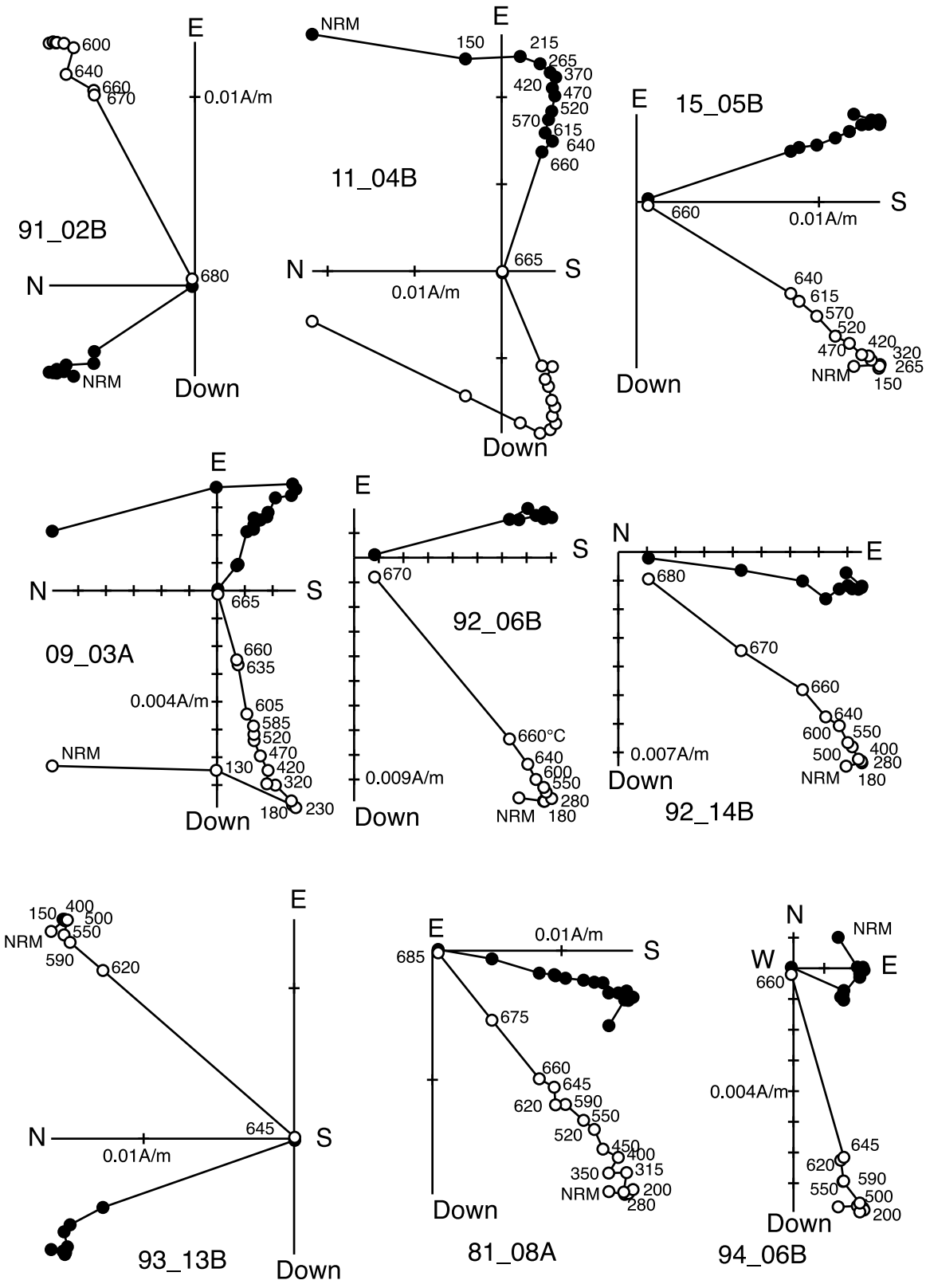

Figure 4. Examples of orthogonal plots of thermal demagnetization for samples of the Soncco and Kayra formations. A characteristic magnetization going through the origin is carried mainly by hematite as shown by high unblocking temperatures above 580°C. Open symbols (filled) correspond to projections in the vertical (horizontal) planes, and all plots are in geographic coordinates.

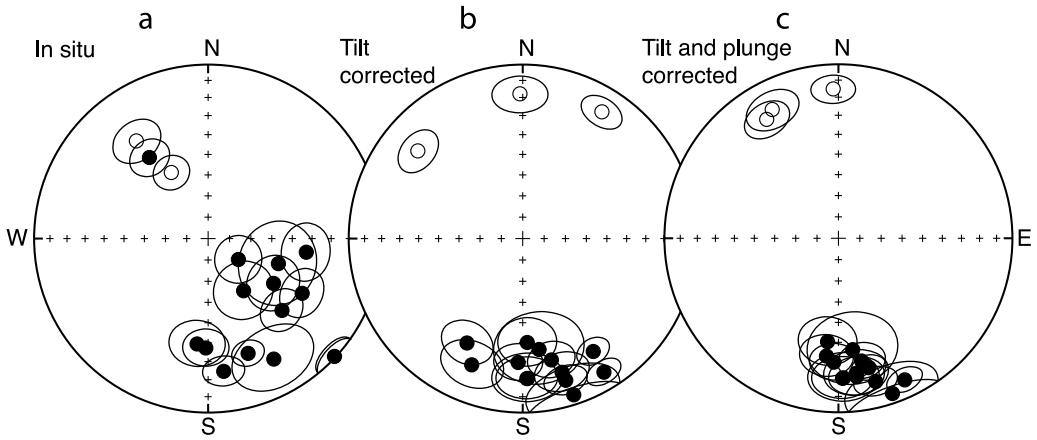

Figure 5. Equal-area stereonets of characteristic directions with 95% confidence angles. Filled (open) symbols are projection in the lower (upper) hemisphere. Data are shown (left) in situ, (center) after conventional bending correction, and (right) after correction of the plunge of the AMS lineation and bedding correction.

the magnetic susceptibility and of the anisotropy in these sediments.

[11] It is well known that thermal enhancement of magnetic susceptibility after heating in the laboratory also enhances the degree of anisotropy (see *Henry et al.*, [2003] for a review). AMS was measured before and after heating for samples of the Kayra formation. A significant increase in the anisotropy up to a degree of 1.5 is observed (Figure 6). There is no change in the orientation of the ellipsoids but the magnetic foliation related to bedding is better defined. The strongly dipping magnetic lineations at some sites are thus unlikely to be due to a complex mineralogy since the same fabric is observed before and after magnetic susceptibility enhancement during heating.

[12] The AMS lineation is well grouped at all sites except at site 2 which is the uppermost site sampled in the Soncco formation and for which the magnetic fabric is mainly oblate (Table 2). The shape of the site-mean AMS ellipsoid varies from oblate at 13 sites to prolate at 3 sites (Figure 7). The bedding-parallel oblate AMS is overprinted by a tectonic fabric as described by *Borradaile and Henry* [1997]. Except at site 94, bedding mainly controls the AMS magnetic foliation but there is a significant dispersion in the azimuth of the magnetic lineations after tilt correction (Figure 7). With in situ coordinates, the magnetic lineation presents a spatial variation from one locality to the other (Figure 8). The magnetic lineation is almost horizontal at sites in locality B (Figure 8) while it is dipping steeply to the west at sites 12 and 13 (locality A, Figure 8) on the western limb of a NS oriented

Table 1. Paleomagnetic Data

					In Situ				Tilt Corrected		AMS Corrected	
Site	Lat	Long	Strike/Dip	l/p/t	Dec	Inc	α95	k	Dec	Inc	Dec	Inc
01	13.60547	−71.86610	135/42	6_0_6	151.4	22.2	16.9	17	161.9	6.2	160.8	6.2
02	13.62203	−71.85766	149/61	12_3_15	134.2	40.5	9.9	16	182.1	29.5	182.1	29.5
08	13.58938	−71.88123	115/51	10_1_11	145.8	60.3	13.8	12	178.0	20.7	177.9	20.8
09	13.59755	−71.87197	126/56	5_0_5	109.6	54.7	19.0	17	171.6	35.8	172.7	35.7
10	13.60195	−71.86627	130/68	10_0_10	120.2	37.5	10.8	21	163.6	21.0	172.5	21.0
11	13.60739	−71.86401	136/72	9_1_10	97.9	42.5	12.5	16	177.5	40.0	186.0	40.0
14	13.72033	−71.68400	14/23	9_0_9	181.2	37.2	9.7	29	166.7	29.1	169.3	29.0
15	13.71763	−71.68121	5/28	10_0_10	173.3	24.2	8.3	35	163.1	16.0	165.4	16.0
16	13.71644	−71.67913	7/36	10_0_10	160.8	30.8	6.8	51	148.7	11.1	154.9	11.1
81	13.72608	−71.68915	56/23	10_0_10	186.0	39.0	11.9	18	178.3	20.6	178.3	20.6
91	13.82315	−71.55553	159/77	11_0_11	330.9	−54.2	8.3	31	32.0	−15.2	358.0	−15.2
92	13.82641	−71.56231	149/80	11_2_13	124.4	52.4	12.7	12	202.0	22.8	172.5	22.8
93	13.82899	−71.56843	152/68	10_2_12	323.7	−31.0	10.6	18	358.9	−17.9	332.8	−17.9
94	13.82534	−71.58494	138/60	9_0_9	124.6	72.8	11.1	23	208.1	32.5	185.8	32.5
12	13.56819	−72.02808	179/84	12_2_14	324.1	42.0	9.0	21/19	309.9	−22.5	328.9	−21.3
13	13.57381	−72.04169	160/64	16_0_16	133.0	0.8	7.8	23/29	148.0	24.5	166.8	24.6
Mean				16	144.5	38.6	15.5	7				
Mean				16			10.3	14	172.8	24.3		
Mean				16			6.3	35			169.9	23.1

[a]Lat, Long, latitude and longitude of the site; strike/dip, strike and dip of bedding measured with the right hand rule; l, p, t, number of lines, planes (t = l + p) used to calculate the mean direction; Dec, Inc, α95, k, the declination, inclination, angle of confidence at 95%, and Fisher parameter. AMS corrected indicates that a double correction rotating first the AMS lineation to the horizontal was applied.

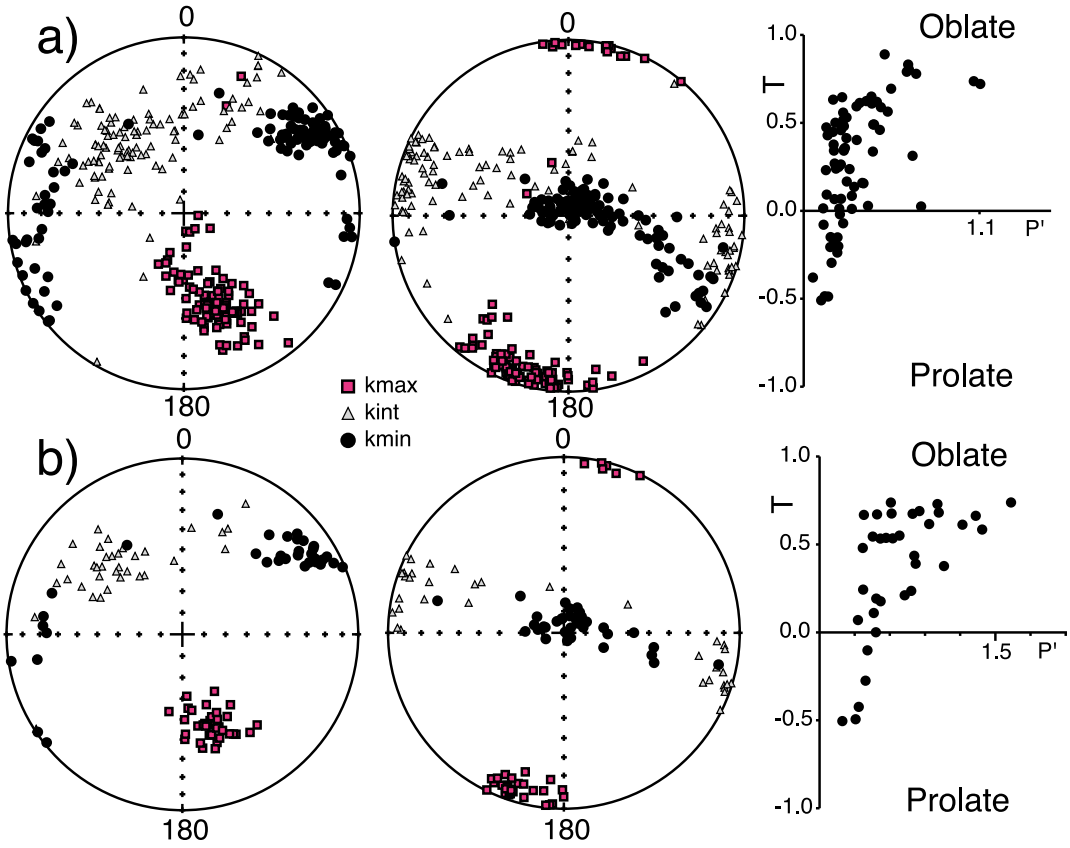

Figure 6. Stereonets projection of principal directions of the AMS ellipsoids for (a) nonheated and (b) heated samples from the Kayra formation in situ and after tilt correction and corresponding T-P′ diagrams.

anticline. West of Urcos, the magnetic lineation is dipping nearly 20° toward the south-southeast (Locality C, Figure 8) and the lineation is steeper (about 40°) near Quiquijana (locality D, Figure 8).

4. Discussion

[13] Several paleomagnetic studies have focused on the effect of increasing strain on the remanent magnetization [*Vetter et al.*, 1989] and on the magnetic fabric. For the latter, there has been no attempt to check the importance of rigid rotation posterior to the magnetic fabric acquisition. If the magnetic lineation is acquired during the first stages of folding, the lineation may behave like a passive marker and register rotations around vertical and horizontal axes unless there is a significant increase in strain capable to modify internally the magnetic fabric [*Cogné*, 1988, *Hrouda*, 1991]. In most studies of weakly deformed sediments, the magnetic foliation related to sedimentary processes register a rigid rotation during folding and a classic bedding correction is usually applied to the AMS fabric in order to present the data in a common reference frame. If the magnetic lineation is horizontal and parallel to the strike of bedding as it is usually the case for LPS lineations, applying the bedding correction does not change the orientation of the magnetic lineation.

[14] In our present study, the magnetic lineation is not always horizontal and paleocurrents directions were determined at some sites to test the hypothesis that magnetic lineations may be controlled by hydrodynamic condition during deposition. At sites 91 to 94, paleocurrents indicate transport to the ENE while the magnetic lineation is oriented to the south ruling out a sedimentary origin for the magnetic lineation.

[15] The sediments are only folded with fracture cleavage but without pervasive schistosity. The deformation is not strong enough to reset the initial magnetic foliation related to bedding and all sites but sites 91, 12 and 14 exhibit an oblate magnetic fabric parallel to bedding and correspond to type II and type III classes from *Robion et al.* [2007]. The magnetic lineation is contained within the bedding plane but the lineation is however not horizontal in geographic coordinates. In stratigraphic coordinates, AMS lineations appear to cluster in nearly two orthogonal directions (NW-SE and NNE-SSW). *Mattei et al.* [1997] found that magnetic lineations coincide with the stretching directions in extensional basins. Thus, orthogonal groups of lineations could be found if one group of lineations is associated with extension while the other is related to LPS. The Cusco red beds were deposited in compressional synsedimentary basins during the Eocene and a stretching origin for one group of lineations is unlikely. *Aubourg et al.* [1999] also found groups of orthogonal magnetic lineations in Late Jurassic shales from the French Alps and they argue that lineations parallel to the shortening

Table 2. AMS Data[a]

		Kmax									Kmin							Intensity			Shape				
Site	N	Kmax	Dg	Ig	Ds	Is	Ds2	Is2	p1	p2	Kmin	Dg	Ig	Ds	Is	p1	p2	lin	fol	ani	k	t	form	r	P′
12	28	1.028	293.4	73.5	94.9	4.6	115.1	10.1	4.9	1.7	0.975	83.9	14.4	320.6	83.5	7.5	4.2	1.030	1.024	1.055	1.253	−0.11	p	1.054	1.055
13	26	1.018	294.8	48.5	97.7	5.0	116.7	5.2	9.9	4.4	0.972	62.6	28.5	317.9	83.4	5.2	2.6	1.009	1.038	1.048	0.236	0.61	o	1.047	1.051
01	8	1.023	133.4	2.7	135.6	3.1	135.0	3.3	6.0	3.7	0.966	40.1	50.7	272.6	85.8	4.7	1.5	1.012	1.046	1.059	0.268	0.57	o	1.059	1.063
02	19	1.021	307.9	35.5	288.5	2.1	288.7	1.2	14.6	3.3	0.964	55.6	23.2	34.5	82.5	3.5	2.5	1.006	1.053	1.059	0.104	0.81	o	1.059	1.065
08	13	1.015	114.4	0.1	114.6	0.5	114.6	0.5	8.3	2.6	0.981	24.3	41.6	222.4	88.3	3.6	3.1	1.010	1.024	1.035	0.415	0.41	o	1.034	1.036
09	10	1.017	299.8	2.2	119.8	2.1	121.4	3.0	17.0	3.3	0.979	31.2	32.4	351.5	86.6	9.3	3.2	1.012	1.025	1.038	0.494	0.34	o	1.038	1.039
10	14	1.017	304.8	13.3	295.8	0.3	304.9	−0.1	9.2	1.5	0.974	39.5	19.1	31.1	87.1	2.7	1.0	1.009	1.036	1.044	0.244	0.60	o	1.044	1.047
11	20	1.034	318.1	11.6	305.6	5.5	314.3	5.1	6.3	4.0	0.942	51.8	17.5	132.1	84.5	4.5	2.3	1.010	1.086	1.097	0.117	0.78	o	1.096	1.107
14	15	1.008	143.1	20.3	140.2	2.2	143.0	1.8	8.4	4.6	0.994	240.2	18.5	231.7	34.3	39.7	7.9	1.011	1.003	1.014	3.701	−0.57	p	1.014	1.014
15	15	1.022	130.6	15.3	309.4	7.5	311.8	7.9	8.0	4.2	0.972	260.4	66.9	138.1	82.4	8.0	6.3	1.016	1.035	1.052	0.446	0.38	o	1.051	1.053
16	18	1.011	141.3	27.8	134.9	0.7	141.3	0.3	5.1	2.4	0.987	282.3	55.8	35.1	86.0	5.3	4.8	1.009	1.016	1.025	0.545	0.29	o	1.024	1.025
81	19	1.016	146.8	21.6	326.8	0.4	146.8	−1.0	7.3	3.5	0.982	316.9	68.1	230.0	86.6	11.3	2.7	1.015	1.020	1.035	0.739	0.15	o	1.035	1.035
91N	14	1.010	161.2	44.0	201.7	6.7	168.5	7.4	4.0	2.1	0.990	260.7	9.7	97.7	64.0	15.3	2.6	1.011	1.009	1.020	1.160	−0.07	p	1.020	1.020
91D	10	1.078	160.9	42.1	199.8	6.5	166.5	7.2	4.5	2.8	0.925	70.2	0.9	78.2	77.7	19.8	3.0	1.081	1.078	1.165	1.043	−0.02	p	1.158	1.165
92N	14	1.007	149.1	35.2	183.0	4.9	154.3	5.7	5.6	4.2	0.992	240.0	1.3	68.2	78.5	9.8	4.0	1.007	1.008	1.015	0.877	0.07	o	1.015	1.015
92D	5	1.092	151.8	35.4	183.5	2.7	154.9	3.5	14.3	1.7	0.872	53.4	11.7	307.1	85.1	22.2	10.5	1.054	1.187	1.252	0.288	0.53	o	1.241	1.265
93N	27	1.011	161.4	39.1	190.8	6.1	165.4	6.8	7.3	2.6	0.985	55.5	18.6	3.2	83.8	4.7	2.1	1.007	1.019	1.026	0.359	0.47	o	1.026	1.027
93D	12	1.077	164.7	41.1	193.7	4.6	168.3	5.3	6.1	4.1	0.884	55.9	20.2	350.7	85.0	8.4	3.0	1.036	1.176	1.219	0.206	0.64	o	1.213	1.235
94N	17	1.017	195.3	68.9	215.8	11.6	196.5	11.8	6.4	3.9	0.976	287.4	0.8	120.4	24.9	10.2	3.8	1.010	1.031	1.042	0.329	0.50	o	1.041	1.043
94D	8	1.077	173.8	52.3	197.6	4.5	178.1	4.9	9.4	7.7	0.919	43.0	26.8	359.1	85.2	24.3	8.5	1.074	1.091	1.172	0.817	0.10	o	1.165	1.172

[a]N, number of specimens measured for each site. The directions of the Kmax and Kmin axes are given in geographic coordinates (Dg, Ig) and after bedding correction (Ds, Is). Ds2, Is2, declination and inclination of Kmax after a double correction rotating first the AMS lineation to the horizontal; p1,p2, the angles for the ellipses of confidence after *Jelínek and Kropáček* [1978]; Lin, fol, ani, the lineation, foliation, and anisotropy degree; o, p, the oblate or prolate shape of the ellipsoids; K, t, r, P′, the shape parameters. For sites 91, 92, 93, and 94, the letters D and N of the site number indicate whether the samples were heated in the laboratory (D) or not (N).

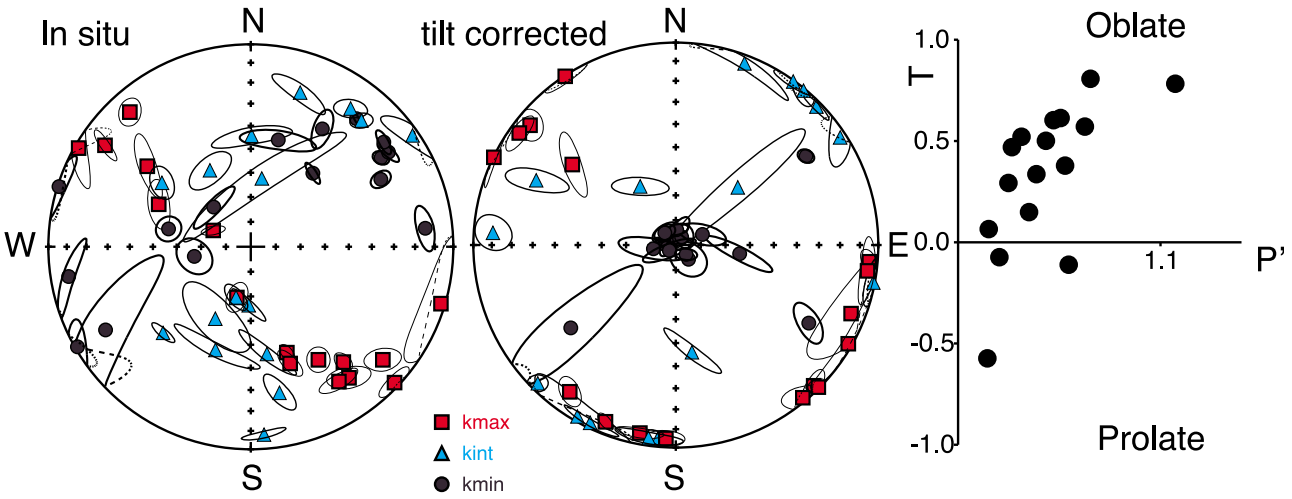

Figure 7. Plots of the site-mean AMS tensors with 95% error ellipses in situ and after bedding correction and T-P′ diagrams.

direction may be related to a simple shear mechanism in the direction of tectonic transport. *Saint-Bezar et al.* [2002] also found orthogonal lineations due to hematite recrystallization in open cracks parallels to the shortening direction. We do not think that these types of magnetic fabrics are present in our data. First, as shown in Figure 8, the magnetic lineation is coherently grouped by locality with sites separated by 1 to three kilometers recording a similar magnetic fabric and the average dip of the lineation varies from near horizontal to steeply inclined from one locality to the other. A simple shear mechanism in the direction of tectonic transport is thus unlikely. On the other hand, the orientation of the magnetic fabric is not correlated with a specific magnetic property. We cannot assign a specific fabric to different ratios of magnetite versus hematite and this observation rules out a mineralogical control in the orientation of the magnetic lineation. In samples from the Kayra formation the orientation of the magnetic fabric is the same in samples without or with heated enhanced fabric.

[16] *Carlotto* [1998] reported two generations of fracture cleavages. The magnetic lineation is close to the intersection of bedding with the first generation of fracture cleavage (Figure 8). This observation demonstrates that the magnetic fabric is indeed associated with the first event of tectonic compression in the area. This result is not unique and other studies [*Soto et al.*, 2003] also reported the conservation of a primary magnetic fabric during subsequent deformation events.

[17] A complex history of folding is shown at locality A (sites 12,13) by the NS trending anticline oblique to the main NW-SE trend of folding observed at locality B (Figure 8). Field observations indicate that the NS anticline corresponds to the most recent phase of folding. In the Bolivian Andes, the deformation started in the Late Eocene mainly along the Eastern Cordillera (see *Oncken et al.*, [2006] for a review). This deformation is coeval with a phase of oroclinal bending registered by undeformed sediments from the south Peruvian forearc [*Roperch et al.*, 2006; *Arriagada et al.*, 2008]. In the southern Peruvian Andes, deposition of the red beds is synchronous with the magmatic activity and the intrusion of the late Eocene Andahuaylas-Yauri batholith to the west of the study area [*Perello et al.*, 2003]. The presence of copper enriched sedimentary layers in the Soncco formation suggests uplift and erosion of some of the late Eocene hydrothermal porphyries within the wide magmatic belt. The syntectonic sedimentary sequence was later further deformed during the Miocene. Miocene deposit of the Paruro formation are folded and overthrusted by the Eocene Oligocene deposits. Moreover, fault scarps [*Cabrera and Sébrier*, 1998] and Quaternary shoshonitic intrusions [*Carlier et al.*, 2005] along some of the major fault systems demonstrate a significant tectonic activity up to recent time.

[18] It is thus very likely that the AMS fabric was mainly acquired during the Oligocene–early Miocene first episode of deformation and that it was later further rotated around vertical or horizontal axes during the mid Miocene to recent phases of deformation in the area.

4.1. Application of a Double Correction

[19] The remanent magnetizations are better grouped after bedding correction than with in situ coordinates but there is a significant variation in declination. An apparent clockwise rotation is observed for the sites near Quiquijana while a counterclockwise rotation is observed at locality A (Figure 5). The same trend is observed in the magnetic lineation after bedding correction (Figure 7). As discussed above, the tilt of the magnetic lineation is likely due to complex folding but as discussed by *MacDonald* [1980], it is not trivial to unravel different phases of folding because tilt corrections are not commutative. Because the magnetic lineation is likely acquired during the first phase of folding, the tilt of the lineation is probably acquired during the second phase of folding. Obviously we do not know exactly how the lineation was tilted and we thus assume that the direction of the lineation is the direction of the tilt. This is the simplest solution but we warn that this may not be always valid. In the present study, the magnetic lineations in geographic coordinates are not

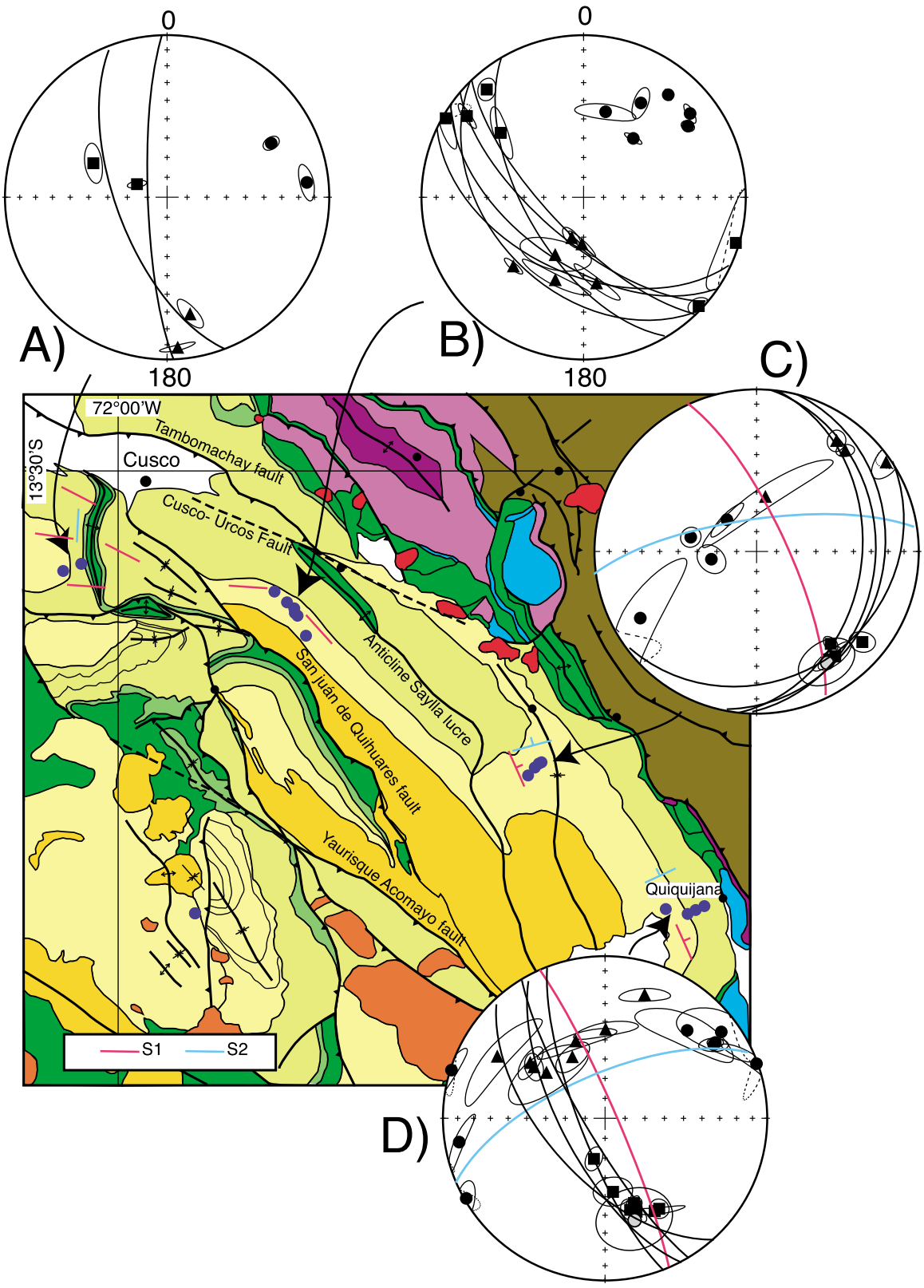

Figure 8. Plots of the site-mean AMS tensors with 95% error ellipses for the four localities. Bedding and fracture cleavages S1 and S2 are shown by black, red, and blue great circles, respectively.

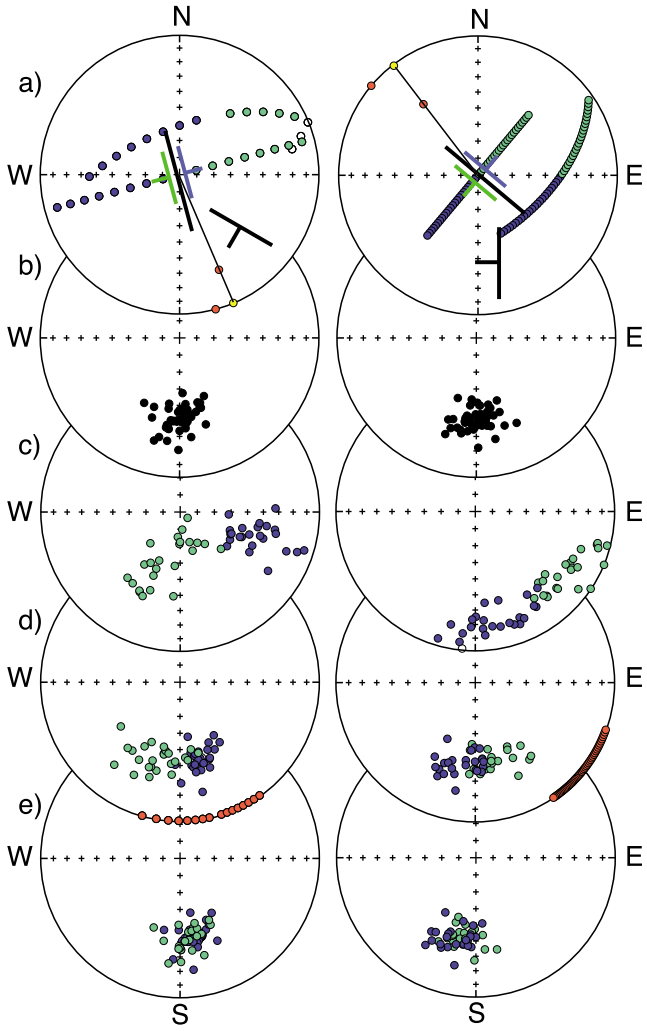

Figure 9. (a) Simulation of the effects of interference of two phases of deformation applied to (b) two data sets of vectors with Fisherian distribution. (left) Example of a fold with different bedding dips of 10° to 80° and tilted toward the southwest by 40°. (right) Example of a fold with dips of 2° to 48° and tilted to the west by 50°. (c) Data given with in situ coordinates. (d) Data after conventional tilt correction with the girdle of red circles corresponding to the fold axis. (e) Data after double corrections that first brings the tilted fold axis (red circle in Figure 9a) to the horizontal (yellow circle in Figure 9a). The green and blue colors illustrate the different behaviors of the two limbs of a fold subjected to a second phase of deformation.

randomly scattered. The distribution of the lineations roughly in a vertical plane supports the hypothesis of a secondary folding phase almost orthogonal to the first stage. A more detailed analysis of the departure of the magnetic lineations from a vertical plane may help better constrain the direction of the secondary folding. In the present study we use the simplest configuration by applying two rotations around horizontal axes. The first rotation brings the magnetic lineation to horizontal around an axis perpendicular to the lineation. This rotation is applied to the pole of bedding and to the characteristic remanent magnetization. The second rotation is the classic tilt correction using the corrected pole of bedding. This second rotation is applied to the magnetic lineation and to the remanent magnetization. The paleomagnetic data are better grouped after this double correction (Figure 5c and Table 1).

[20] To test this method of correction, we simulated two examples of structures recording two phases of deformation with a strong obliqueness (Figure 9). These two examples are close to the structures observed in our study at locality D and locality A.

[21] In the first case (left side in Figure 9), a fold oriented N165 is tilted toward the southwest by 40°. The second structure (right side in Figure 9) corresponds to a fold oriented N310 which is then tilted toward the west by 50°.

[22] The two deformations are applied to a population of data with a Fisherian distribution centered on direction (Dec = 180° Inc = 40°) characterized by a concentration parameter k of 60. We then compare the results using conventional tilt correction (Figure 9d) and a double correction bringing first to the horizontal the fold axis (Figure 9e). The sum of the two rotations results in a plunge of the fold axis to the south in the first case and to the northwest in the second case (Figure 9a).

[23] Simple tilt correction around a horizontal axis leads to clockwise and counterclockwise rotations of paleomagnetic data from the two limbs of the fold and a strong dispersion. A strong dispersion in the fold axes is also observed (Figure 9d). The double correction bringing back the axis of the fold to the horizontal around an axis orthogonal to the fold axis reduces dispersion but induced a component of apparent rotation whose magnitude depends on the angle between the two deformations. The apparent rotation is the angle between the true original orientation of the fold axis and the one after a tilt correction around an orthogonal axis (yellow circles in Figure 9a). These simple examples suggest that if both limbs of a fold can be sampled, the mean direction is not as strongly rotated as if only a single limb was studied.

[24] In the present study, the sampled sites have bedding attitudes toward the west or the southwest but come from different structures. The mean directions after classic tilt correction and after the double correction are not different. This indicates that the double correction is not accompanied by a significant apparent rotation of the whole area associated with the rotation to the horizontal of the AMS lineations.

4.2. Tectonic Rotations

[25] Our paleomagnetic study demonstrates that the Tertiary basin does not rotate significantly ($R = -4.5° \pm 8.4°$) when compared with the reference pole at 40Ma from *Besse and Courtillot* [2002]. A more significant flattening in the inclination is observed ($16.1° \pm 9.60$) but this amount of flattening is systematically observed in Tertiary red beds from the Andes [*Roperch et al.*, 1999, 2000]. *Gilder et al.* [2003] reported variable counterclockwise rotations up to more than 90° from sites in Permian and Jurassic rocks within the fault system limitating the uplifted Paleozoic block and the Eocene-Oligocene basins (Figures 10a and 10b). For example, there is a large variation (>60°) in the magnitude of rotation from nearby sites (sites 842, 843 and 844; see

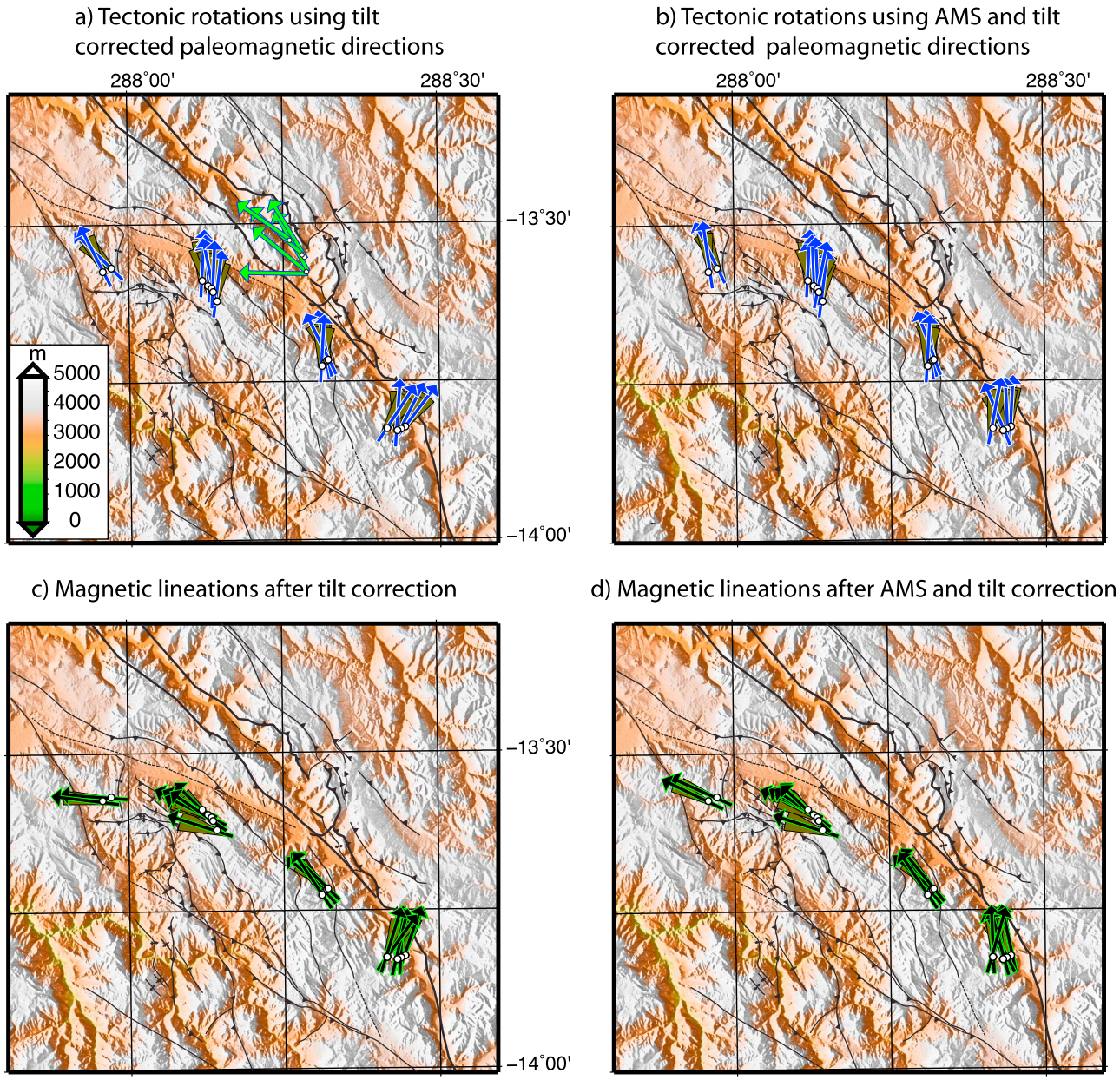

Figure 10. Maps showing apparent tectonic rotations determined after (a) simple tilt correction and (b) double correction rotating first the magnetic lineation to the horizontal. (c and d) Maps showing the magnetic lineations after bedding correction and after double correction, respectively. Green arrows in Figure 10a are tectonic rotations determined by *Gilder et al.* [2003] in Permian to Jurassic rocks. Faults and folds are taken from the geological map of Figure 2. The shaded relief image is from ASTER topography processed with the GMT software.

Figure 2) sampled within the Urcos-Sicuani fault system. The large counterclockwise rotations recorded in Permian to Jurassic rocks [*Gilder et al.*, 2003] likely correspond to local rotations within disrupted thrust sheets and indicate a component of strike-slip shear in the Urcos-Sicuani fault system.

[26] The pattern of orientation of the AMS lineations delineates a curved structure (Figure 10d). The absence of significant tectonic rotation in the area suggests that changes in the orientation of the AMS are mainly controlled by an interplay of the regional stress oriented NW-SE and the orientation of the borders of the two Paleozoic blocks limitating the basins to the east and to the north (Figure 1). In a companion paper (Roperch et al., submitted), large counterclockwise rotations (~60°) were also found in the area a few tens of kilometers to the south of the town of Abancay (Figure 1). The variation in the magnitude of rotation from

Abancay to Cusco demonstrates a complex pattern of block rotation likely associated with sinistral transpression along the Abancay-Cusco deflection.

5. Conclusions

[27] The present Peruvian paleomagnetic study demonstrates the interest of coupling a magnetic fabric study with the study of the remanent magnetization. We show that a magnetic fabric related to the first stages of deformation may not always be reset by following stages of deformation. Tilted AMS lineations are good evidence for complex folding and apparent rotations may be reduced by a double correction that brings the magnetic lineation first to the horizontal. In the present study, the AMS lineations are untilted along an horizontal axis orthogonal to the lineations. This assumption is validated by the reduction of the scatter in the paleomagnetic declination and in the orientation of the AMS lineations but we warn that the proposed correction must be evaluated for each case study especially when the second phase of folding occurred at an angle about 45° from the first phase of folding. The double correction is likely to reduce but will not eliminate all the sources of disturbances in determining tectonic rotations about vertical axes at local and regional scales [see *MacDonald*, 1980; *Waldhör and Appel*, 2009]. Obviously, using the AMS lineation as a proxy of a fold plunge does not apply to highly strained rocks where more complex methods should be used to recover the original orientation of the remanent magnetization [*Cogné and Perroud*, 1985; *Vetter et al.*, 1989; *Borradaile and Hamilton*, 2009].

[28] Other examples where AMS and characteristic directions are reported like the Xishuigou section at Subei [*Gilder et al.*, 2001] confirm that apparent rotations are recorded in the characteristic magnetizations and the AMS lineations. When detailed geological field mapping is not available or not possible, the AMS study is a rapid and easy way to better constrain the tectonic structures and the scatter in the paleomagnetic declination may be reduced with a two-step tilt correction.

[29] **Acknowledgments.** Support for the field work was given by IRD. We would like to thank Philippe Cullerier from Géosciences Rennes for his significant participation in laboratory measurements. P.R. would like to especially thank Jose Berrospi from the IRD office in Peru for his invaluable help in the field. We thank Massimo Mattei and an anonymous referee for their constructive criticism.

References

Arriagada, C., P. Roperch, C. Mpodozis, and P. R. Cobbold (2008), Paleogene building of the Bolivian Orocline: Tectonic restoration of the central Andes in 2-D map view, *Tectonics*, *27*, TC6014, doi:10.1029/2008TC002269.

Aubourg, C., P. Rochette, J.-F. Stephan, M. Popoff, and C. Chabert-Pelline (1999), The magnetic fabric of weakly deformed late Jurassic shales from the Southern Subalpine Chains (French Alps). Evidence for SW-directed transport direction, *Tectonophysics*, *307*, 15–31, doi:10.1016/S0040-1951(99)00116-X.

Aubourg, C., B. Smith, H. Bakhtari, N. Guya, A. Eshragi, S. Lallemant, M. Molinaro, X. Braud, and S. Delaunay (2004), Post-Miocene shortening pictured by magnetic fabric across the Zagros-Makran syntaxis (Iran), *Geol. Soc. Am. Spec. Pap.*, *383*, 17–40.

Aubry, L., P. Roperch, M. De Urreiztieta, E. Rossello, and A. Chauvin (1996), Paleomagnetic study along the south-eastern edge of the Altiplano-Puna Plateau: Neogene Tectonic Rotations, *J. Geophys. Res.*, *101*, 17,883–17,899, doi:10.1029/96JB00807.

Besse, J., and V. Courtillot (2002), Apparent and true polar wander and the geometry of the geomagnetic field over the last 200 Myr, *J. Geophys. Res.*, *107*(B11), 2300, doi:10.1029/2000JB000050.

Borradaile, G. J., and B. Hamilton (2009), Recomputing palaeopoles for the effects of tectonic finite strain, *Tectonophysics*, *467*(1–4), 131–144, doi:10.1016/j.tecto.2008.12.020.

Borradaile, G. J., and B. Henry (1997), Tectonic applications of magnetic susceptibility and its anisotropy, *Earth Sci. Rev.*, *42*(1–2), 49–93, doi:10.1016/S0012-8252(96)00044-X.

Cabrera, J., and M. Sébrier (1998), Surface rupture associated with a 5.3-*mb* earthquake: The 5 April 1986 Cuzco earthquake and kinematics of the Chincheros-Qoricocha faults of the High Andes, Peru, *Bull. Seismol. Soc. Am.*, *88*(1), 242–255.

Carlier, G., J. P. Lorand, J. P. Liégeois, M. Fornari, P. Soler, V. Carlotto, and J. Cardenas (2005), Potassic-ultrapotassic mafic rocks delineate two lithospheric mantle blocks beneath the southern Peruvian Altiplano, *Geology*, *33*, 601–604, doi:10.1130/G21643.1.

Carlotto, V. (1998), Évolution Andine et Raccourcissement au niveau de Cusco (13–16°S) Pérou: Enregistrement sédimentaire, chronologie, controles paléogéographiques, évolution cinématique: unpublished Ph.D. thesis, 159 pp., Univ. Joseph Fourier, Grenoble, France.

Cifelli, F., F. Rossetti, M. Mattei, A. M. Hirt, R. Funiciello, and L. Tortorici (2004), An AMS, structural and paleomagnetic study of Quaternary deformation in eastern Sicily, *J. Struct. Geol.*, *26*(1), 29–46, doi:10.1016/S0191-8141(03)00092-0.

Cifelli, F., M. Mattei, M. Chadima, S. Lenser, and A. M. Hirt (2009), The magnetic fabric in "undeformed clays": AMS and neutron texture analyses from the Rif Chain (Morocco), *Tectonophysics*, *466*, 79–88, doi:10.1016/j.tecto.2008.08.008.

Cogné, J.-P. (1988), Strain, magnetic fabric, and paleomagnetism of the deformed red beds of the Pont-Rean formation, Brittany, France, *J. Geophys. Res.*, *93*, 13,673–13,687, doi:10.1029/JB093iB11p13673.

Cogné, J.-P., and H. Perroud (1985), Strain removal applied to palaeomagnetic directions in an orogenic belt: The Permian red slates of the Alpes Maritimes, France, *Earth Planet. Sci. Lett.*, *72*, 125–140, doi:10.1016/0012-821X(85)90122-0.

Coutand, I., A. Chauvin, P. R. Cobbold, P. Gautier, and P. Roperch (1999), Vertical axis rotations across the Puna plateau (northwestern Argentina) from paleomagnetic analysis of Cretaceous and Cenozoic rocks, *J. Geophys. Res.*, *104*(B10), 22,965–22,984, doi:10.1029/1999JB900148.

Fisher, R. (1953), Dispersion on a sphere, *Proc. R. Soc. A*, *217*, 295–305, doi:10.1098/rspa.1953.0064.

Fornari, M., M. Mamani, I. Ibarra, and G. Carlier (2002), Datación del período volcánico "Tacaza" en el Altiplano de Perú y Bolivia, paper presented at *XI Congreso Peruano de Geología*, Soc. Geol. del Perú, Lima, Peru, 25–28 September.

Frizon de Lamotte, D., C. Souque, S. Grelaud, and P. Robion (2002), Early record of tectonic magnetic fabric during inversion of a sedimentary basin. Short review and examples from the Corbières transfer zone (France), *Bull. Soc. Geol. Fr.*, *173*, 461–469, doi:10.2113/173.5.461.

Gilder, S., Y. Chen, and S. Sen (2001), Oligo-Miocene magnetostratigraphy and rock magnetism of the Xishuigou section, Subei (Gansu Province, western China) and implications for shallow inclinations in central Asia, *J. Geophys. Res.*, *106*, 30,505–30,521, doi:10.1029/2001JB000325.

Gilder, S., S. Rousse, D. Farber, T. Sempere, V. Torres, and O. Palacios (2003), Post-Middle Oligocene origin of paleomagnetic rotations in Upper Permian to Lower Jurassic rocks from northern and southern Peru, *Earth Planet. Sci. Lett.*, *210*, 233–248, doi:10.1016/S0012-821X(03)00102-X.

Graham, J. W. (1966), Significance of magnetic anisotropy in Appalachian sedimentary rocks, in *The Earth Beneath the Continents*, *Geophys. Monogr.*, vol. 10, edited by J. S. Steinhart and T. J. Smith, pp. 627–648, AGU, Washington, D. C.

Henry, B., D. Jordanova, N. Jordanova, C. Souque, and P. Robion (2003), Anisotropy of magnetic susceptibility of heated rocks, *Tectonophysics*, *366*(3–4), 241–258, doi:10.1016/S0040-1951(03)00099-4.

Hrouda, F. (1991), Models of magnetic anisotropy variations in sedimentary thrust sheets, *Tectonophysics*, *185*(3–4), 203–210, doi:10.1016/0040-1951(91)90444-W.

Huang, B. C., Y. C. Wang, T. Liu, T. S. Yang, Y. A. Li, D. J. Sun, and R. X. Zhu (2004), Paleomagnetism of Miocene sediments from the Turfan basin, northwest China: No significant vertical-axis rotation during Neotectonic compression within the Tian Shan Range, Central Asia, *Tectonophysics*, *384*(1–4), 1–21, doi:10.1016/j.tecto.2004.01.003.

Jelínek, V., and V. Kropáček (1978), Statistical processing of anisotropy of magnetic susceptibility measured on group of specimen, *Stud. Geophys. Geod.*, *22*, 50–62, doi:10.1007/BF01613632.

Kissel, C., E. Barrier, C. Laj, and T. Q. Lee (1986), Magnetic fabric in undeformed marine clays from compressional zones, *Tectonics*, *5*, 769–781, doi:10.1029/TC005i005p00769.

MacDonald, W. D. (1980), Net tectonic rotation, apparent tectonic rotation, and the structural tilt correction in paleomagnetism, *J. Geophys. Res.*, *85*(B7), 3659–3669, doi:10.1029/JB085iB07p03659.

Mattei, M., L. Sagnotti, C. Faccenna, and R. Funiciello (1997), Magnetic fabric of weakly deformed clay-rich sediments in the Italian peninsula: Relationship with compressional and extensional tectonics, *Tectonophysics*, *271*, 107–122, doi:10.1016/S0040-1951(96)00244-2.

Oncken, O., D. Hindle, J. Kley, K. Elger, P. Victor, and K. Schemmann (2006), Deformation of the central Andean upper plate system: Facts, fiction, and constraints for plateau models, in *The Andes*, *Frontiers Earth Sci.: Part I*, edited by O. Oncken et al., pp. 3–28, Springer, New York.

Paquereau, P., M. Fornari, P. Roperch, J-C. Thouret, and O. Macedo (2008), Paleomagnetism, magnetic fabric, and 40Ar/39Ar dating of Pliocene and Quaternary ignimbrites in the Arequipa area, southern Peru, *Bull. Volcanol.*, *70*, 977–997.

Pares, J. M., B. A. van der Pluijm, and J. DinarËs-Turell (1999), Evolution of magnetic fabrics during incipient deformation of mudrocks (Pyrenees, northern Spain): Applications of magnetic anisotropies to fabric studies of rocks and sediments, *Tectonophysics*, *307*(1–2), 1–14, doi:10.1016/S0040-1951(99)00115-8.

Perello, J., V. Carlotto, A. Zarate, P. Ramos, H. Posso, and A. Caballero (2003), Porphyry-Style Alteration and Mineralization of the Middle Eocene to Early Oligocene Andahuaylas-Yauri Belt, Cusco Region, Peru, *Econ. Geol.*, *98*, 1575–1605, doi:10.2113/98.8.1575.

Perroud, H., and P. R. Cobbold (1984), L'aimantation rémanente comme marqueur de la déformation: Exemple d'un pli à axe incliné dans les séries rouges siluro-dévoniennes à Cabrillanes, Asturies (Espagne), *Bull. Soc. Geol. Fr.*, *26*, 169–184.

Rees, A. I. (1965), The use of anisotropy of magnetic susceptibility in the estimation of sedimentary fabric, *Sedimentology*, *4*, 257–271, doi:10.1111/j.1365-3091.1965.tb01550.x.

Robion, P., D. F. de Lamotte, C. Kissel, and C. Aubourg (1995), Tectonic versus mineralogical contribution to the magnetic fabrics of epimetamorphic slaty rocks: An example from the Ardennes Massif (France-Belgium), *J. Struct. Geol.*, *17*(8), 1111–1124, doi:10.1016/0191-8141(95)00002-U.

Robion, P., S. Grelaud, and D. Frizon de Lamotte (2007), Pre-folding magnetic fabrics in fold-and-thrust belts: Why the apparent internal deformation of the sedimentary rocks from the Minervois basin (NE–Pyrenees, France) is so high compared to the Potwar basin (SW–Himalaya, Pakistan)?, *Sediment. Geol.*, *196*(1–4), 181–200, doi:10.1016/j.sedgeo.2006.08.007.

Rochette, P., M. Jackson, and C. Aubourg (1992), Rock magnetism and the interpretation of anisotropy of magnetic susceptibility, *Rev. Geophys.*, *30*, 209–226, doi:10.1029/92RG00733.

Roperch, P., G. Herail, and M. Fornari (1999), Magnetostratigraphy of the Miocene Corque basin, Bolivia: Implications for the geodynamic evolution of the Altiplano during the late Tertiary, *J. Geophys. Res.*, *104*, 20,415–20,429.

Roperch, P., M. Fornari, G. Hérail, and G. V. Parraguez (2000), Tectonic rotations within the Bolivian Altiplano: Implications for the geodynamic evolution of the central Andes during the late Tertiary, *J. Geophys. Res.*, *105*, 795–820, doi:10.1029/1999JB900311.

Roperch, P., T. Sempere, O. Macedo, C. Arriagada, M. Fornari, C. Tapia, M. García, and C. Laj (2006), Counterclockwise rotation of late Eocene–Oligocene fore-arc deposits in southern Peru and its significance for oroclinal bending in the central Andes, *Tectonics*, *25*, TC3010, doi:10.1029/2005TC001882.

Sagnotti, L., A. Winkler, P. Montone, L. Di Bella, F. Florindo, M. T. Mariucci, F. Marra, L. Alfonsi, and A. Frepoli (1999), Magnetic anisotropy of Plio-Pleistocene sediments from the Adriatic margin of the northern Apennines (Italy): Implications for the time-space evolution of the stress field, *Tectonophysics*, *311*(1–4), 139–153, doi:10.1016/S0040-1951(99)00159-6.

Saint-Bezar, B., R. L. Hebert, C. Aubourg, P. Robion, R. Swennen, and D. Frizon de Lamotte (2002), Magnetic fabric and petrographic investigation of hematite-bearing sandstones within ramp-related folds: Examples from the South Atlas Front (Morocco), *J. Struct. Geol.*, *24*, 1507–1520, doi:10.1016/S0191-8141(01)00140-7.

Soto, R., M. Mattei, and A. M. Casas (2003), Relationship between AMS and folding in an area of superimposed folding (Cotiella-Buixols nappe, southern Pyrenees), *Geodin. Acta*, *16*(2–6), 171–185.

Soto, R., J. C. Larrasoaa, L. E. Arlegui, E. Beamud, B. Oliva-Urcia, and J. L. Simun (2009), Reliability of magnetic fabric of weakly deformed mudrocks as a palaeostress indicator in compressive settings, *J. Struct. Geol.*, *31*(5), 512–522, doi:10.1016/j.jsg.2009.03.006.

Vetter, J. R., Jr., K. P. Kodama, and A. Goldstein (1989), Reorientation of remanent magnetism during tectonic fabric development: An example from the Waynesboro formation, Pennsylvania, U.S.A, *Tectonophysics*, *165*(1–4), 29–39, doi:10.1016/0040-1951(89)90033-4.

Waldhör, M., and E. Appel (2009), Layer parallelisation: An unrecognized mechanism for palaeomagnetic rotations in fold belts, *Tectonophysics*, *474*(3–4), 516–525, doi:10.1016/j.tecto.2009.04.028.

Weaver, R., A. P. Roberts, R. Flecker, and D. I. M. Macdonald (2004), Tertiary geodynamics of Sakhalin (NW Pacific) from anisotropy of magnetic susceptibility fabrics and paleomagnetic data, *Tectonophysics*, *379*(1–4), 25–42, doi:10.1016/j.tecto.2003.09.028.

V. Carlotto, INGEMMET, Av. Canada 1470, San Borja, Lima 41, Peru. (vcarlotto@ingemmet.gob.pe)

A. Chauvin and P. Roperch, Géosciences Rennes, campus de Beaulieu, F-35042 Rennes, France. (annick.chauvin@univ-rennes1.fr; pierrick.roperch@ird.fr)